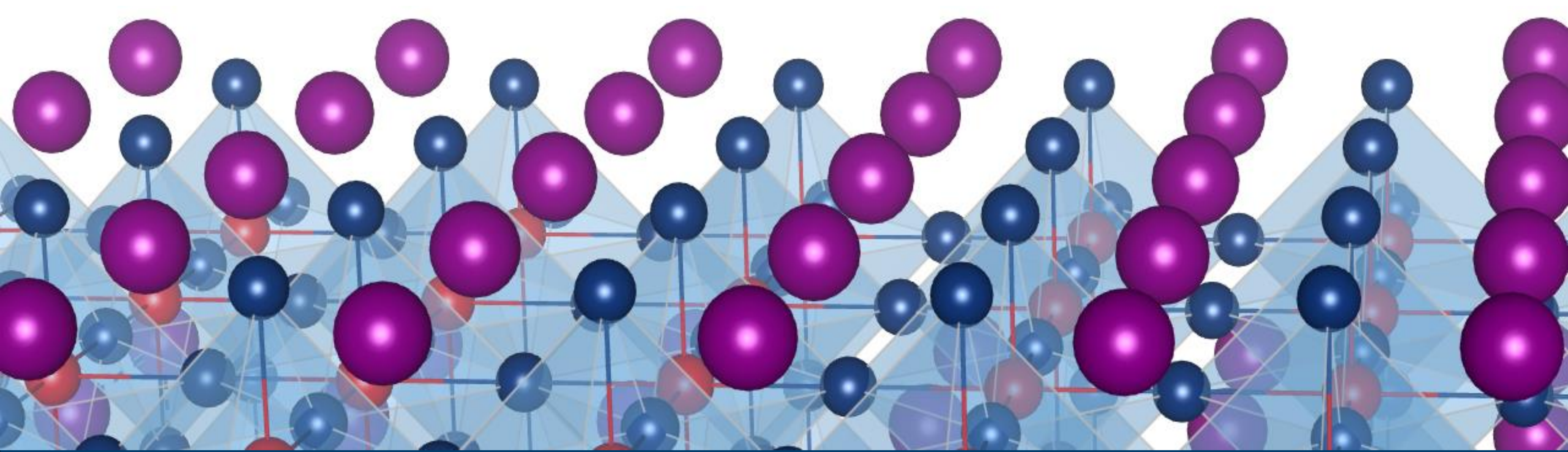

A MULTILAYER MODEL TO UNDERSTAND THE CAPACITANCE RESPONSE OF PEROVSKITE SOLAR CELLS

Sandheep Ravishankar[1], Thomas Kirchartz[1,2]

[1]IEK-5 Photovoltaik, Forschungszentrum Jülich,

[2]NST and CENIDE, Universität Duisburg-Essen

HELMHOLTZ RESEARCH FOR GRAND CHALLENGES

JÜLICH Forschungszentrum

overview

1. Discussion of capacitance methods commonly used to characterise perovskite solar cells –

- Capacitance-voltage (CV) profiling
- Mott-Schottky plots and doping profiles
- Thermal admittance spectroscopy (TAS) measurements
- Time domain transients

2. Interpretation of the high or intermediate frequency (non-ionic) capacitance response of perovskite solar cells in these methods using a multilayer capacitance model.

depletion region capacitance

band bending determined by Poisson equation

$$\frac{d^2V}{dx^2} = -\frac{q}{\varepsilon_r \varepsilon_0}\left[N_D^+(x) - N_A^+(x)\right]$$

dopant/trap densities

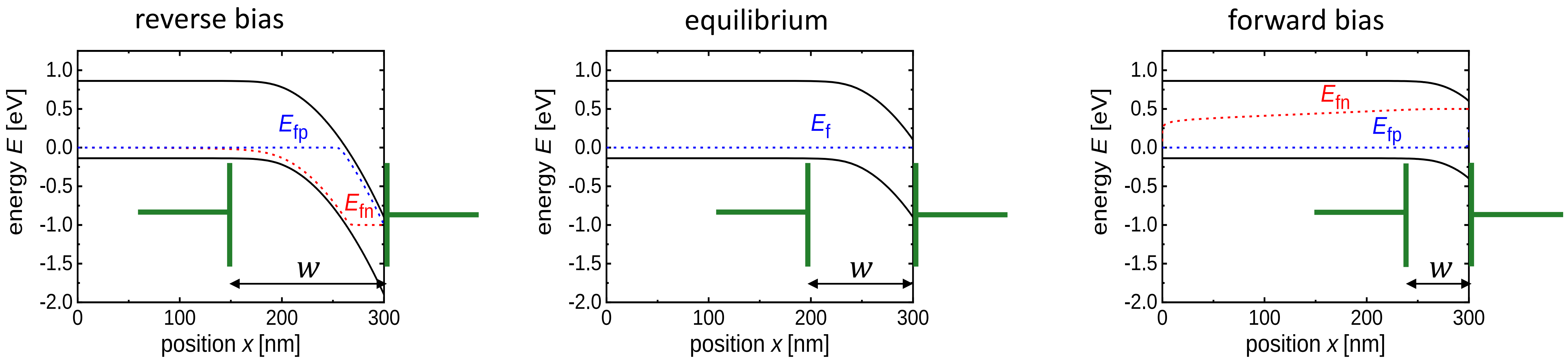

$$C(V) = \frac{\epsilon_r \epsilon_0}{w(V)}$$

Mott-Schottky plot and doping profile

$$C(V) = \sqrt{\frac{q\epsilon_r\epsilon_0 N_D}{2(V_{bi} - V)}} \qquad C^{-2}(V) = \frac{2}{q\epsilon_r\epsilon_0 N_D}(V_{bi} - V) \qquad N_D(V) = \frac{-2(dC^{-2}/dV)^{-1}}{q\epsilon_r\epsilon_0}$$

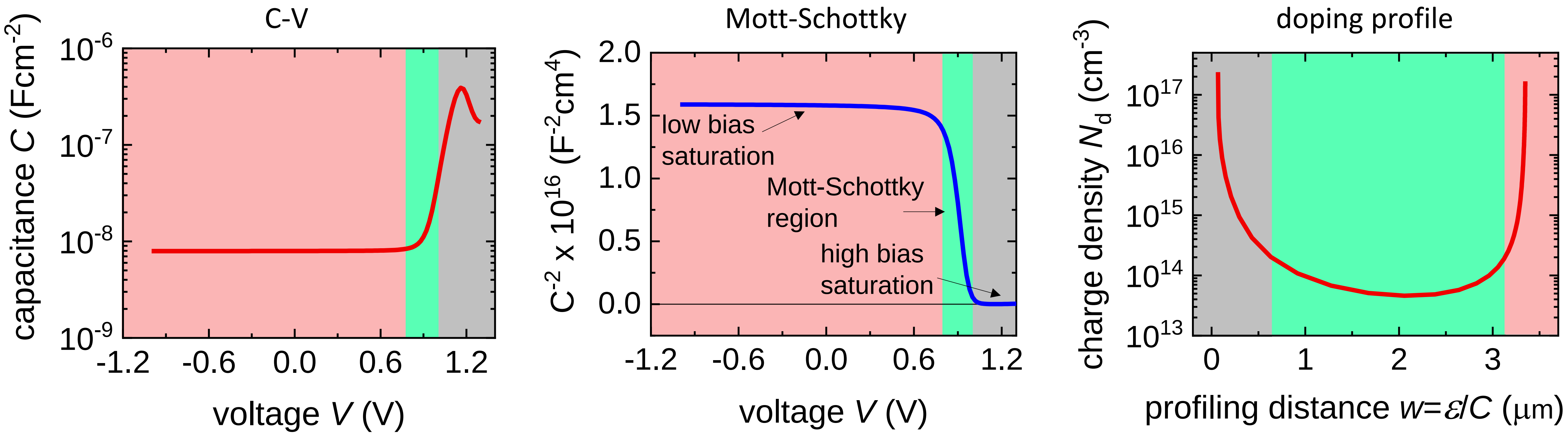

provides important parameters – doping/trap density, built-in voltage, Debye length

perovskite Mott-Schottky plots

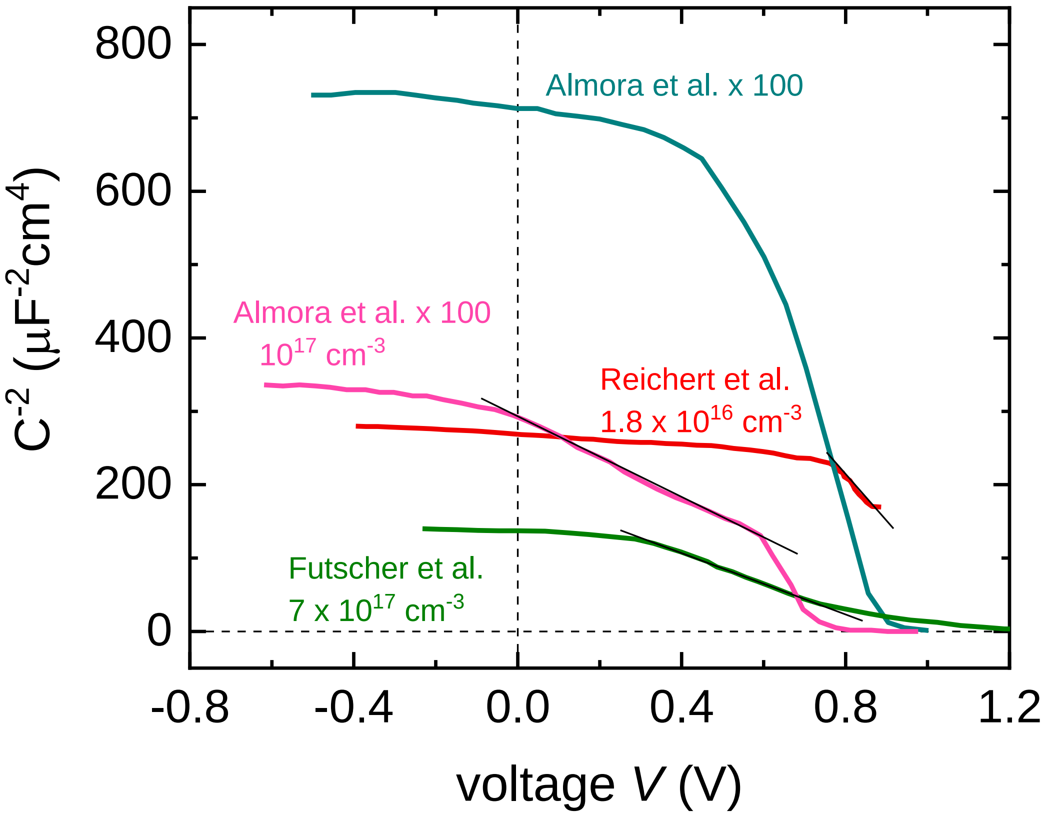

reported doping densities between 10^{16}-10^{18} cm^{-3}

Almora, O. et al., 2016. *Applied Physics Letters*, *109*(17), p.173903.
Futscher, M.H. et al., 2020. *The Journal of Chemical Physics*, *152*(4), p.044202.
Reichert, S. et al., 2020. *Physical Review Applied*, *13*(3), p.034018.

doped or intrinsic?

luminescence data, Kirchartz et al., 2020

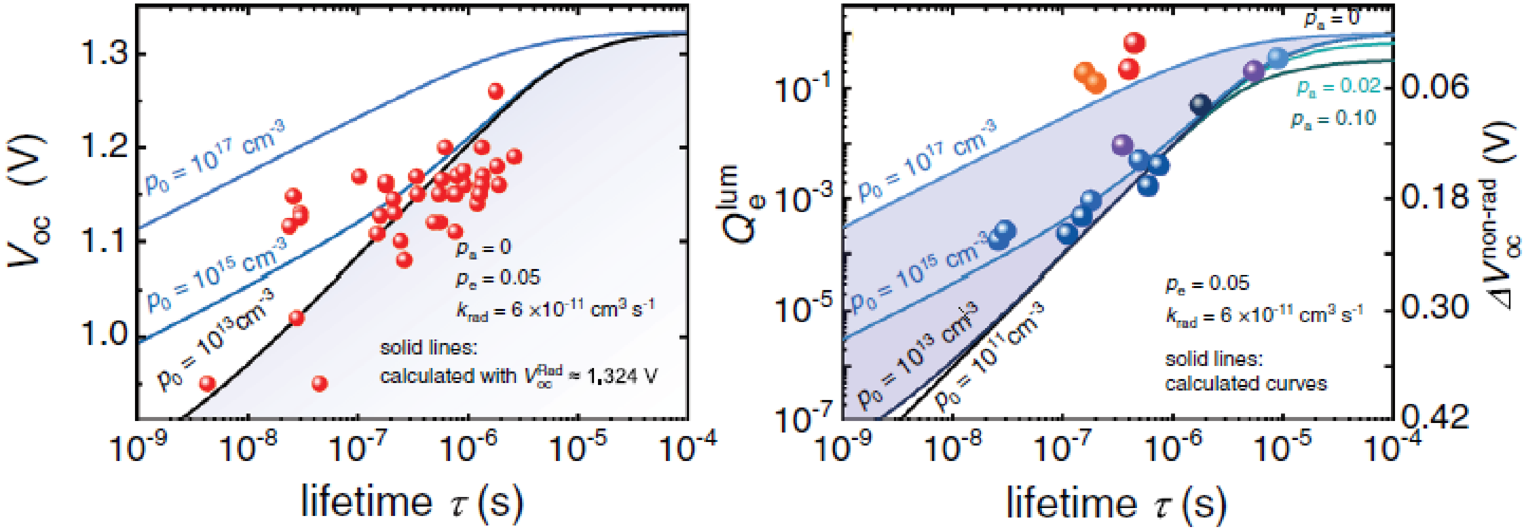

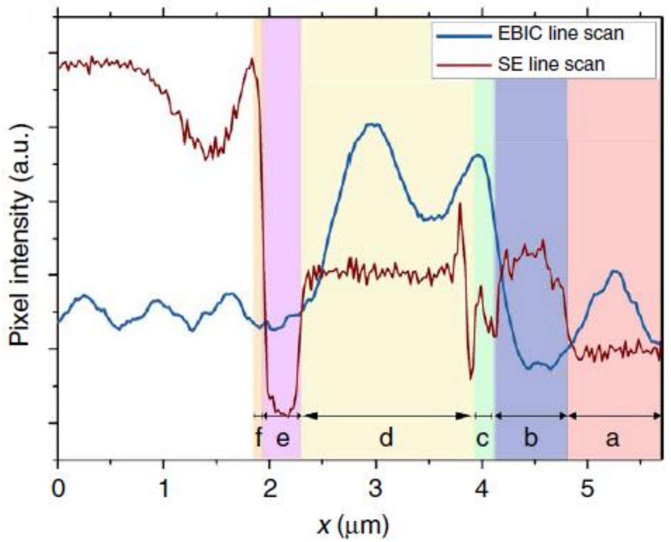

EBIC measurements
Edri et al., 2014

some evidence of intrinsic perovskites

Edri, E., Kirmayer, S., Mukhopadhyay, S., Gartsman, K., Hodes, G. and Cahen, D., 2014. *Nature communications*, *5*(1), pp.1-8.
Kirchartz, T., Márquez, J.A., Stolterfoht, M. and Unold, T., 2020. *Advanced energy materials*, *10*(26), p.1904134.

perovskite Mott-Schottky plots

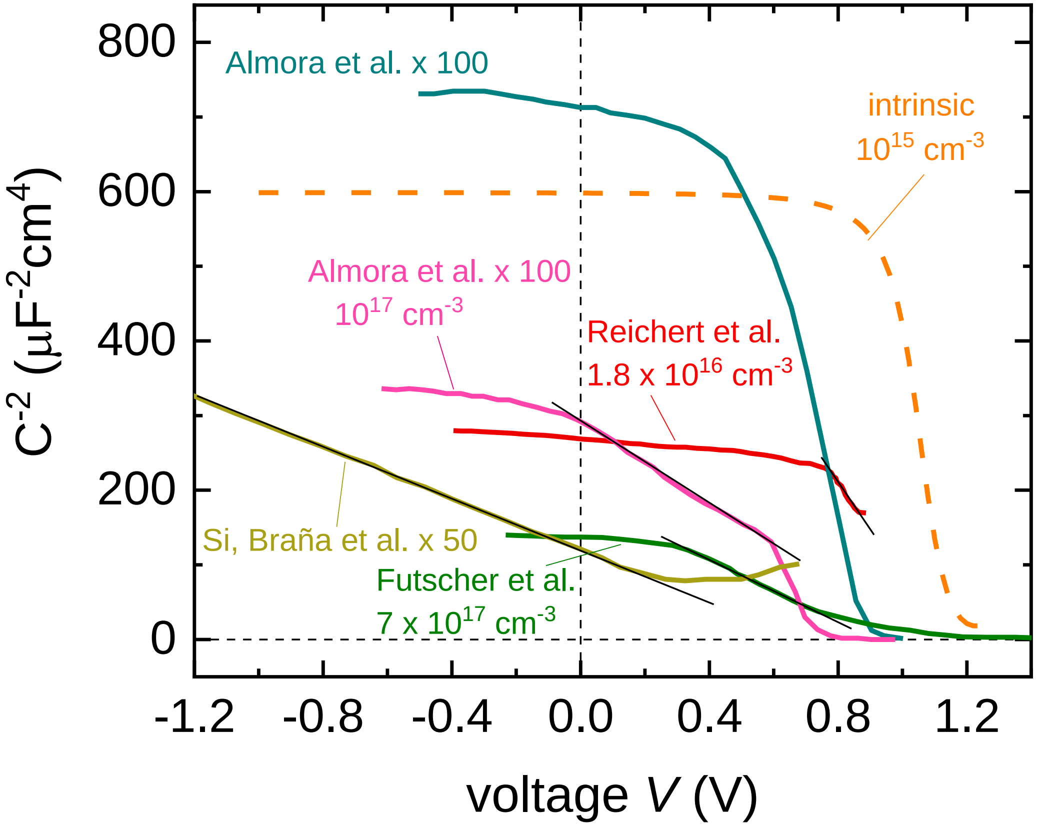

why does an intrinsic semiconductor make an apparent Mott-Schottky behaviour at forward bias?

Almora, O. et al., 2016. *Applied Physics Letters*, *109*(17), p.173903.
Futscher, M.H. et al., 2020. *The Journal of Chemical Physics*, *152*(4), p.044202.
Reichert, S. et al., 2020. *Physical Review Applied*, *13*(3), p.034018.

Braña, A.F. et al., 2015. In *Journal of Physics: Conference Series* (Vol. 647, No. 1, p. 012069).

chemical capacitance

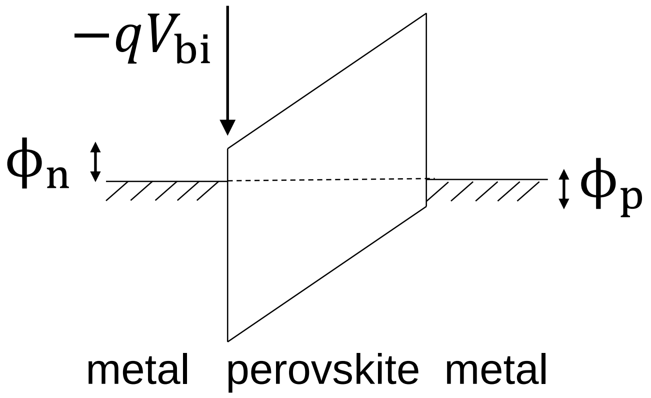

$$C_\mu = C_0 \exp\frac{qV}{mk_BT}$$

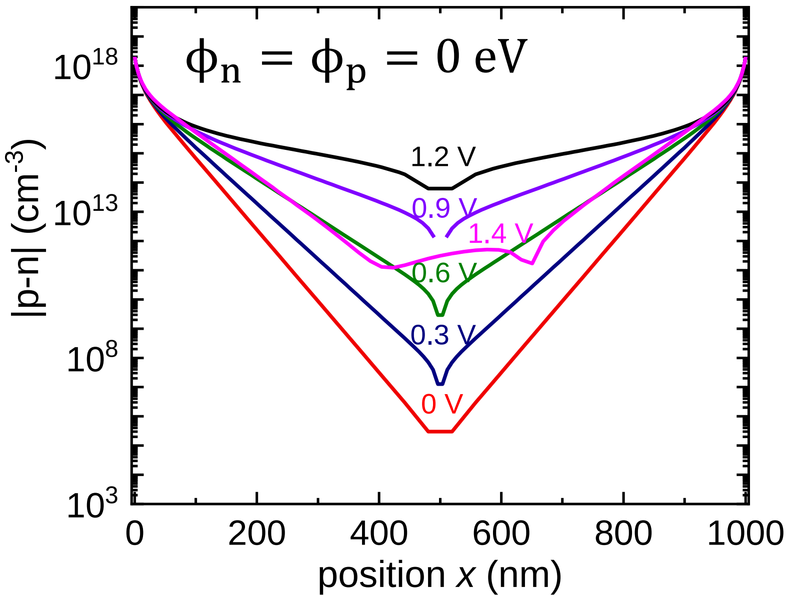

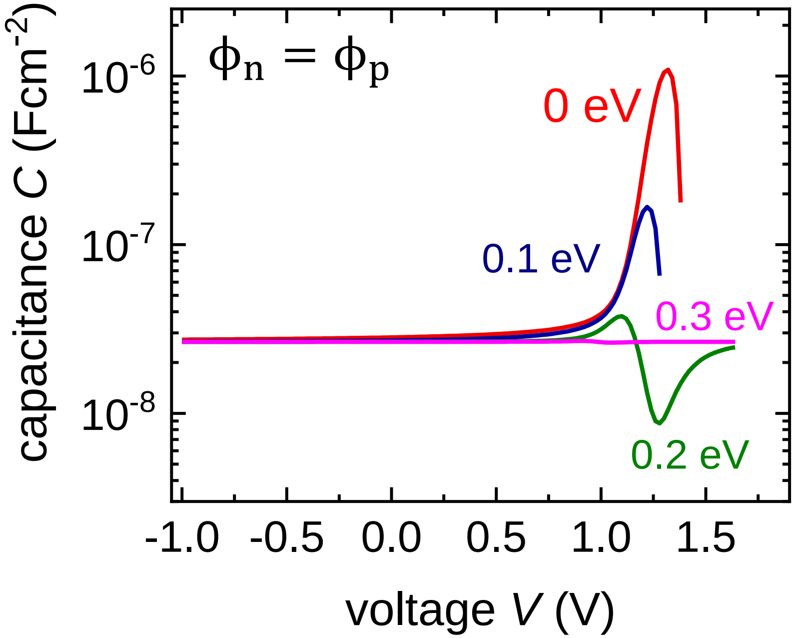

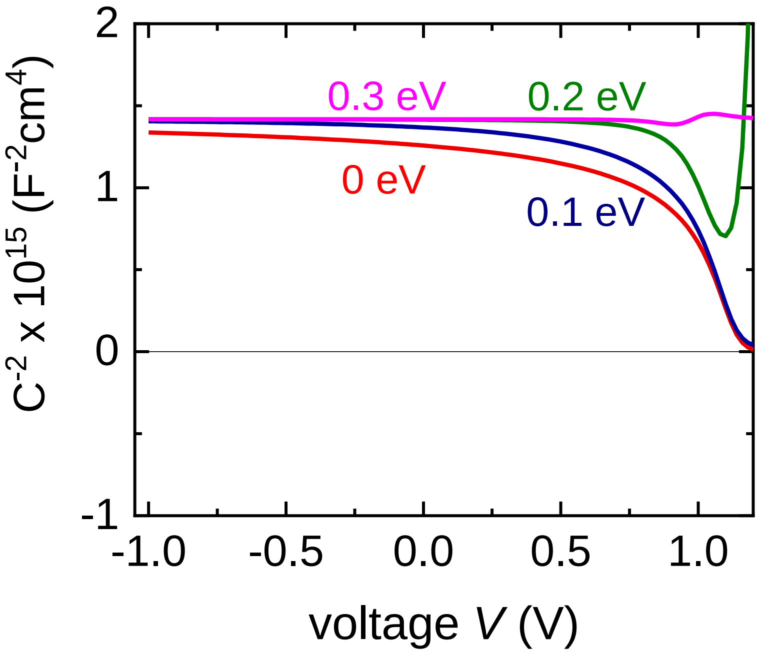

multilayer capacitances

Si solar cell

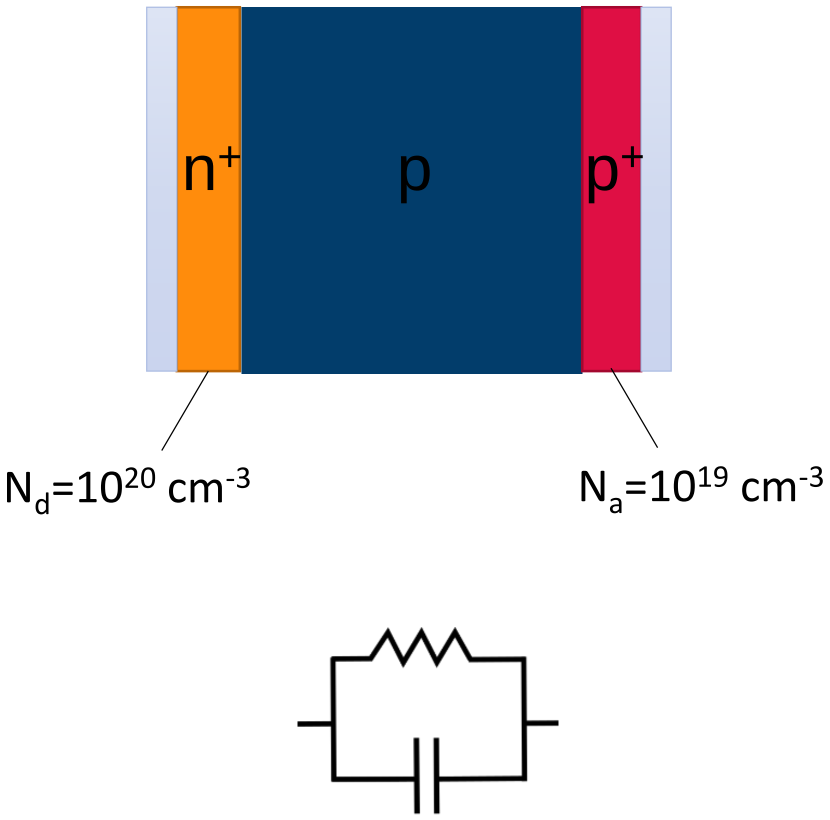

perovskite solar cell

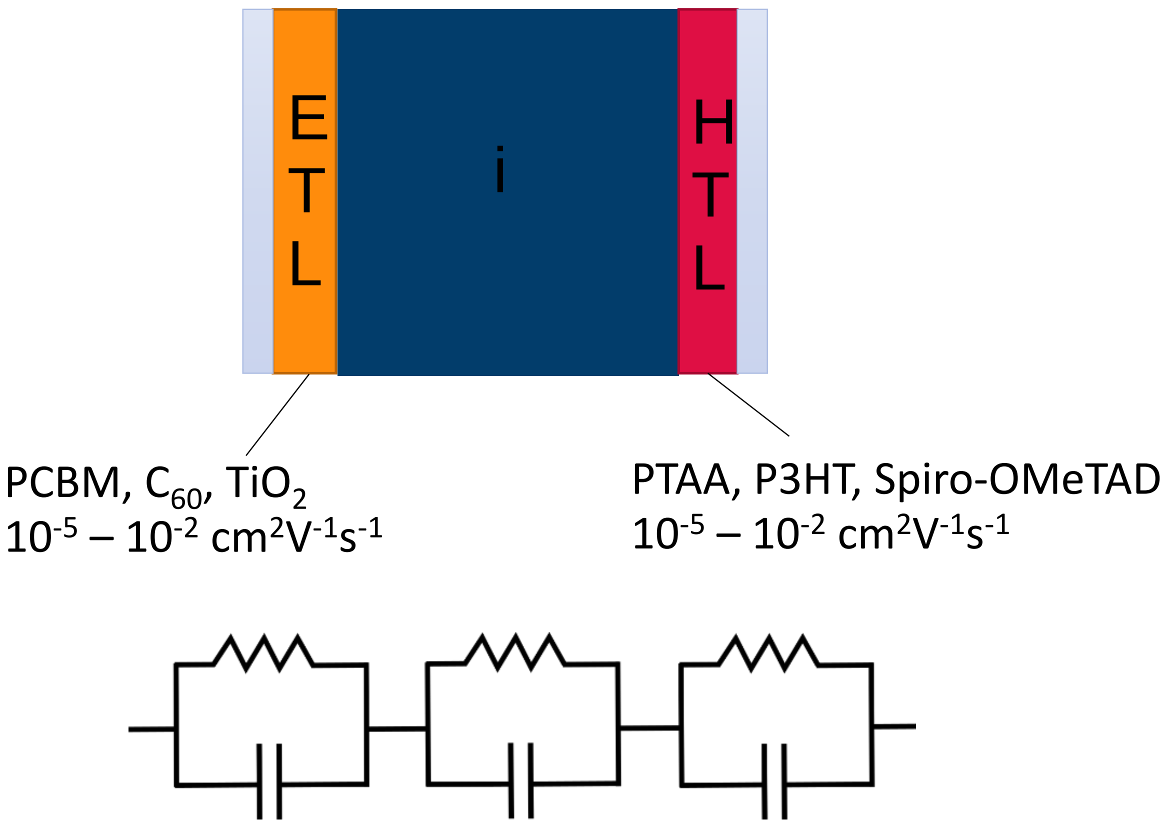

capacitances of the selective contacts cannot be neglected, due to their resistances

multilayer capacitance model

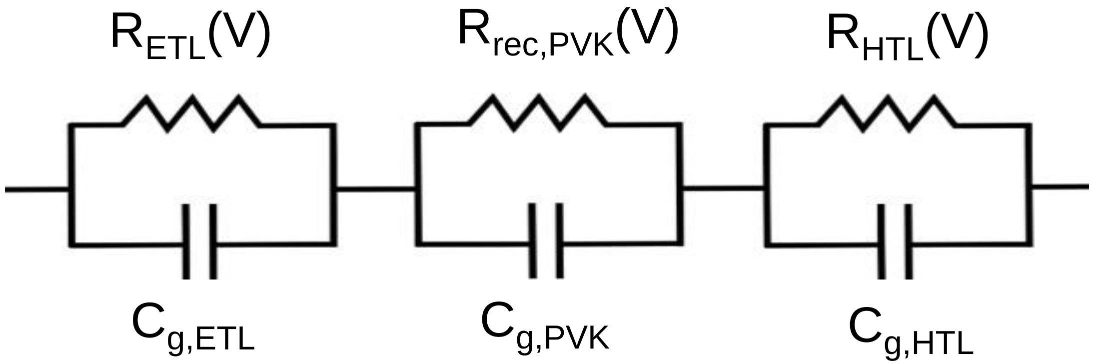

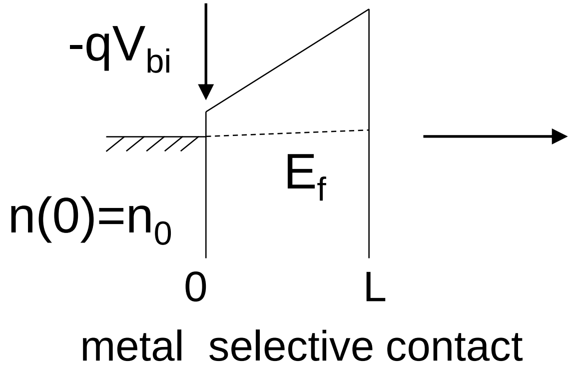

$$R_{\mathrm{ETL/HTL}}(V) = \frac{1}{L}\int_0^L \frac{L}{\sigma(x)}dx = \frac{L}{q\mu n_0(\frac{q(V_{\mathrm{bi}}-V)}{mk_{\mathrm{B}}T})}[\exp\left(\frac{q(V_{\mathrm{bi}}-V)}{mk_{\mathrm{B}}T}\right)-1]$$

$$\propto \exp(\frac{q(V_{\mathrm{bi}}-V)}{n_{\mathrm{ID}}k_{\mathrm{B}}T})$$

$$C_{net}(V) = \frac{1}{i\omega Z_{\mathrm{net}}} = (\frac{i\omega R_{\mathrm{ETL}}}{1+\frac{i\omega}{\omega_{\mathrm{ETL}}}} + \frac{i\omega R_{\mathrm{rec,PVK}}}{1+\frac{i\omega}{\omega_{\mathrm{PVK}}}} + \frac{i\omega R_{\mathrm{HTL}}}{1+\frac{i\omega}{\omega_{\mathrm{HTL}}}})^{-1}$$

$$\omega_{\mathrm{char}} = \frac{1}{RC}$$

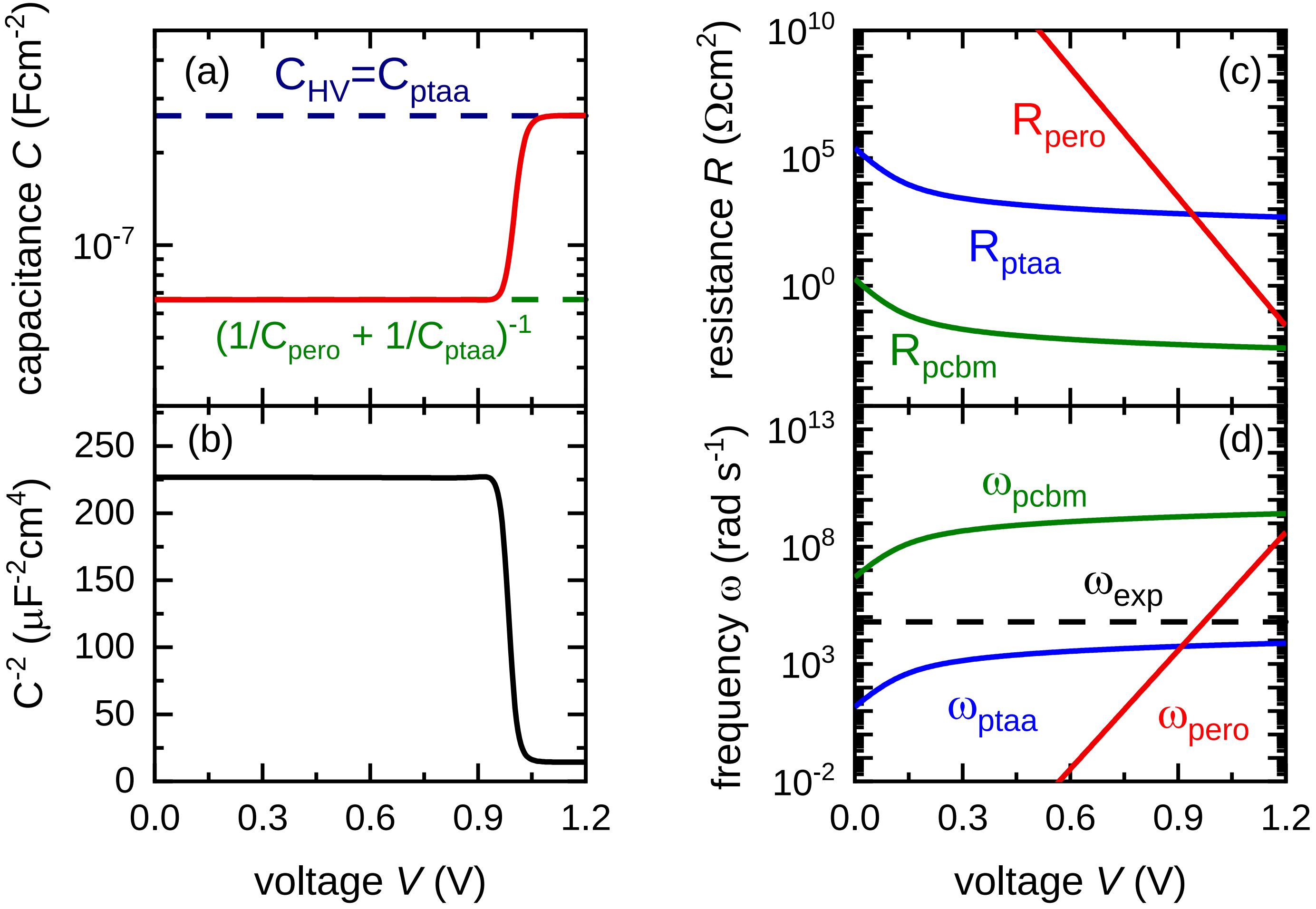

magnitude of characteristic frequency in comparison to experiment frequency determines which capacitance will be expressed at a given voltage multilayer model + chemical capacitance

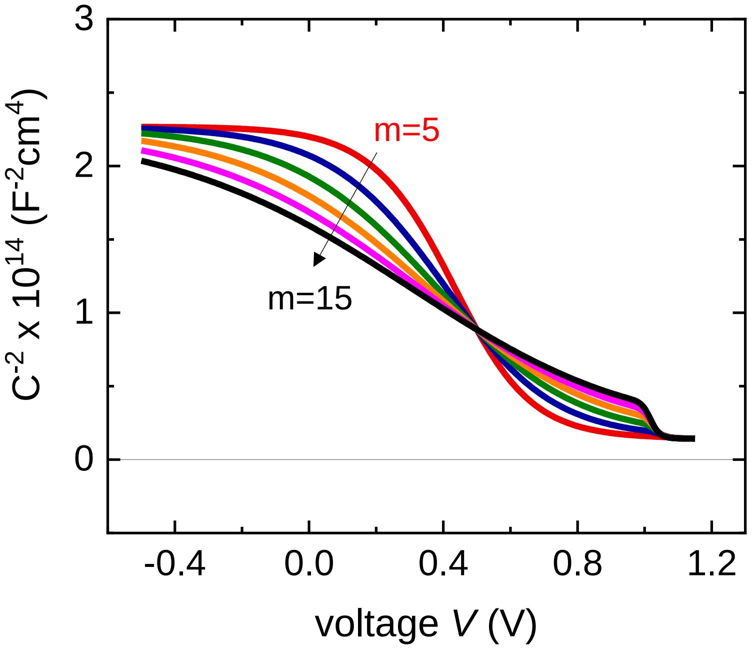

capacitance-voltage

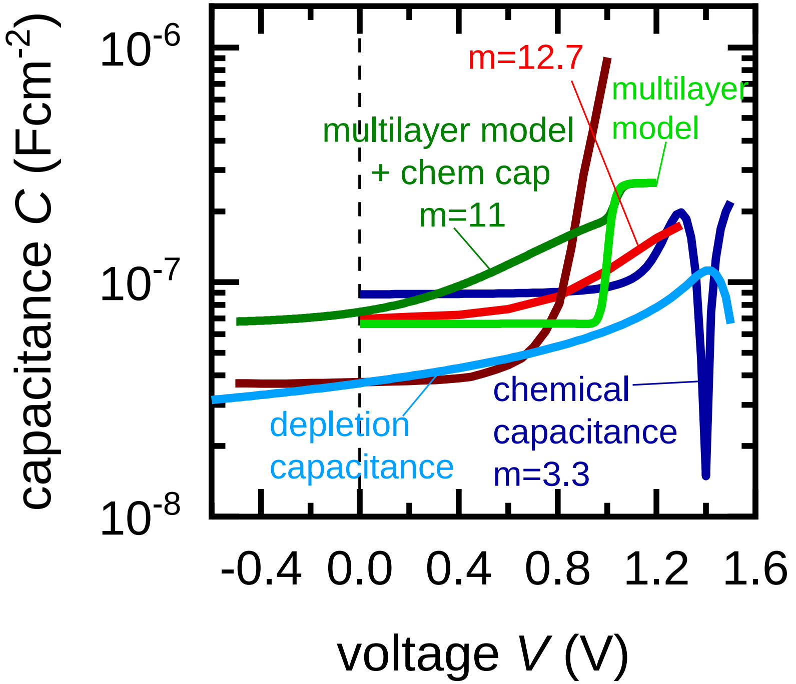

forward bias yields general capacitance evolution of the form

$$C(V) = C_g + C_0 \exp\frac{qV}{mk_BT}$$

depletion capacitance can be resolved only at reverse bias

Mott-Schottky formalism of general capacitance

$$C(V) = C_g + C_0 \exp \frac{qV}{mk_B T} \longrightarrow N_{d,min} = \frac{27 m k_B T \epsilon_r \epsilon_0}{4q^2 d^2}$$

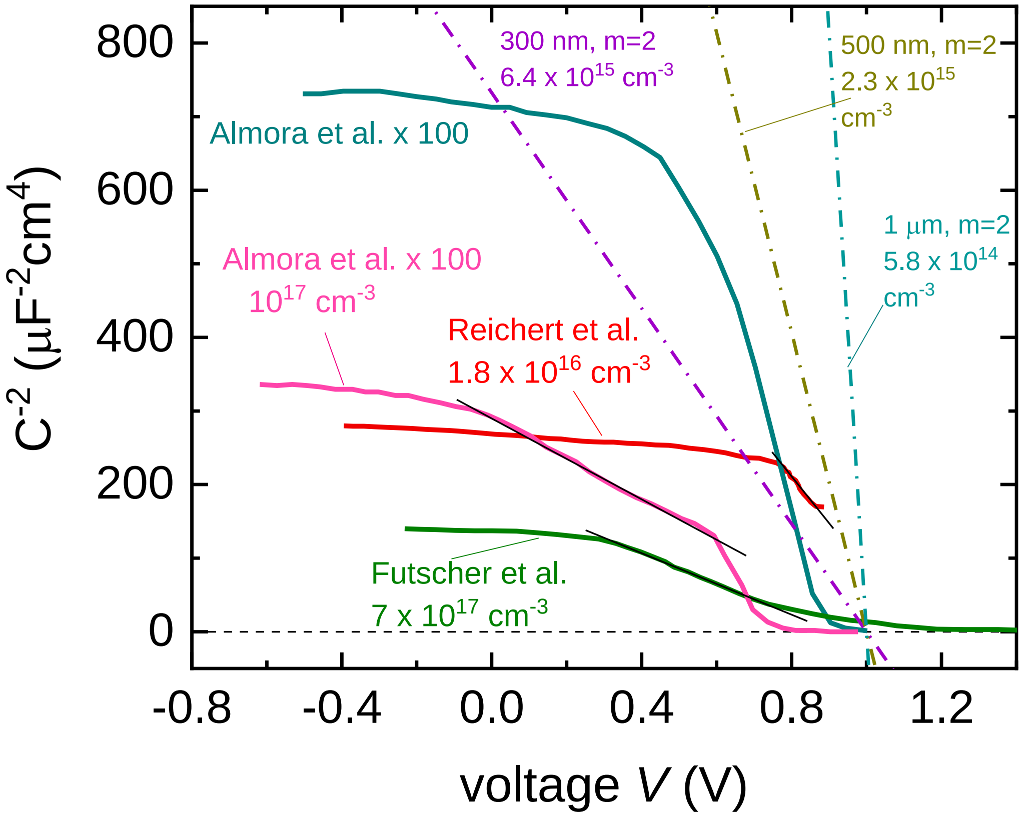

- charge injection + multilayer capacitance transitions cause a minimum charge density to be observed
- in this limit, thin films always show higher apparent trap/doping densities compared to bulk single crystals

Ravishankar, S., Unold, T. and Kirchartz, T., 2021. Comment on “Resolving spatial and energetic distributions of trap states in metal halide perovskite solar cells”. *Science*, *371*(6532).

doping profiles of PSCs

drive-level capacitance profiling (DLCP)

$$Q(\bar{V}+\tilde{V}) = \frac{d\bar{Q}}{d\bar{V}}\tilde{V} + \left(\frac{d^2\bar{Q}}{2d\bar{V}^2}\right)\tilde{V}^2 + \cdots$$

$$C = \frac{d\tilde{Q}}{d\tilde{V}} = C_0 + C_1\tilde{V} + \cdots$$

CV

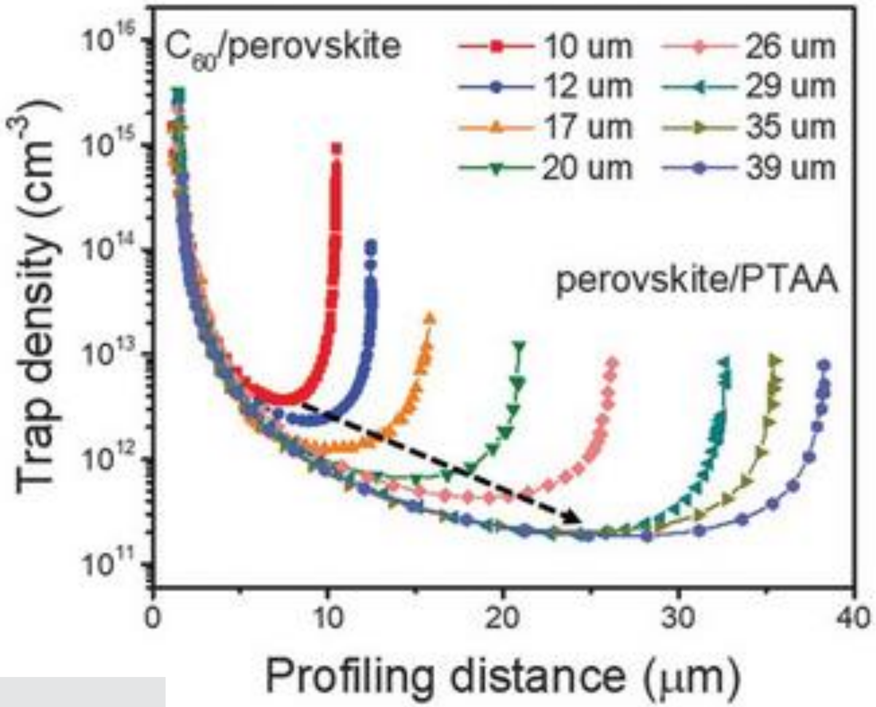

Perovskite material	Minimal bulk trap density ($N_{T\,min}$) (cm^{-3})	Interface trap density (cm^{-3})	
$MAPbBr_3$ single crystal (bulk)	6.5×10^{10}	1.8×10^{12} (C_{60})	1.8×10^{12} (Au)
$MAPbI_3$ single crystal (bulk)	1.8×10^{11}	1.2×10^{12} (C_{60})	1.2×10^{12} (Au)
$MAPbI_3$ single crystal (thin)	1.9×10^{11} to 3.2×10^{12}	2.0×10^{13} to 1.1×10^{16} (C_{60})	1.5×10^{13} to 1.0×10^{15} (PTAA)
$Cs_{0.05}FA_{0.70}MA_{0.25}PbI_3$ film	4.3×10^{14}	8.6×10^{15} (C_{60})	1.2×10^{17} (PTAA)
$Rb_{0.05}Cs_{0.05}FA_{0.75}MA_{0.15}Pb(I_{0.95}Br_{0.05})_3$ film	5.7×10^{14}	2.0×10^{16} (C_{60})	1.1×10^{17} (PTAA)
$FA_{0.92}MA_{0.08}PbI_3$ film	7.9×10^{14}	1.9×10^{16} (C_{60})	9.0×10^{16} (PTAA)
$MAPbI_3$ film	9.2×10^{14}	2.2×10^{16} (C_{60})	1.2×10^{17} (PTAA)
$Cs_{0.05}FA_{0.8}MA_{0.15}Pb_{0.5}Sn_{0.5}(I_{0.85}Br_{0.15})_3$ film	1.2×10^{15}	1.5×10^{16} (C_{60})	1.1×10^{17} (PTAA)

Ni, Z. et al., 2020. Resolving spatial and energetic distributions of trap states in metal halide perovskite solar cells. *Science*, *367*(6484), pp.1352-1358.

DLCP

SCAPS, dopant and trap-free PSC

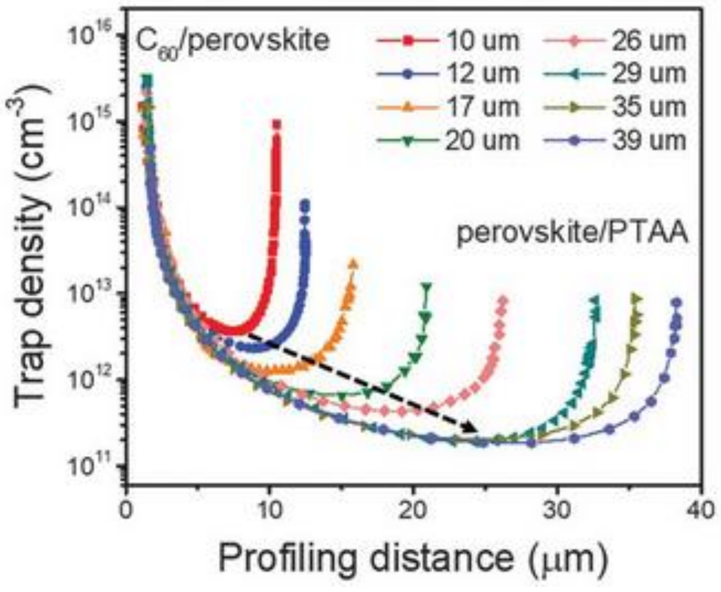

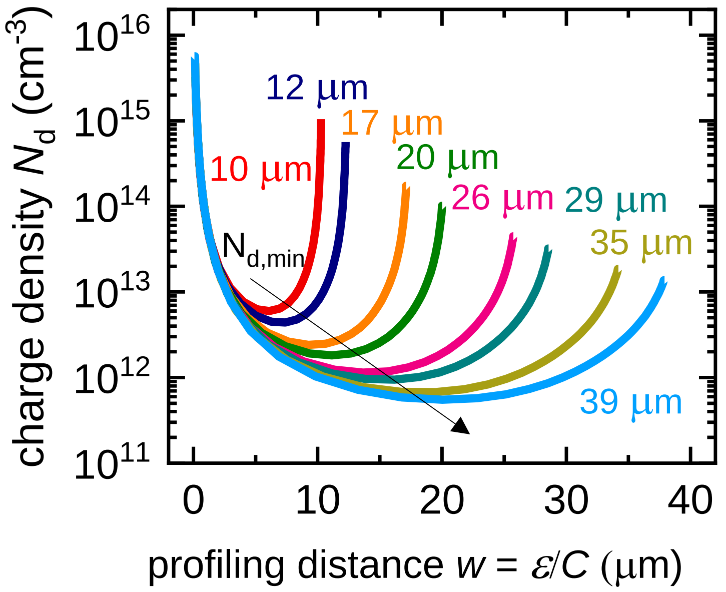

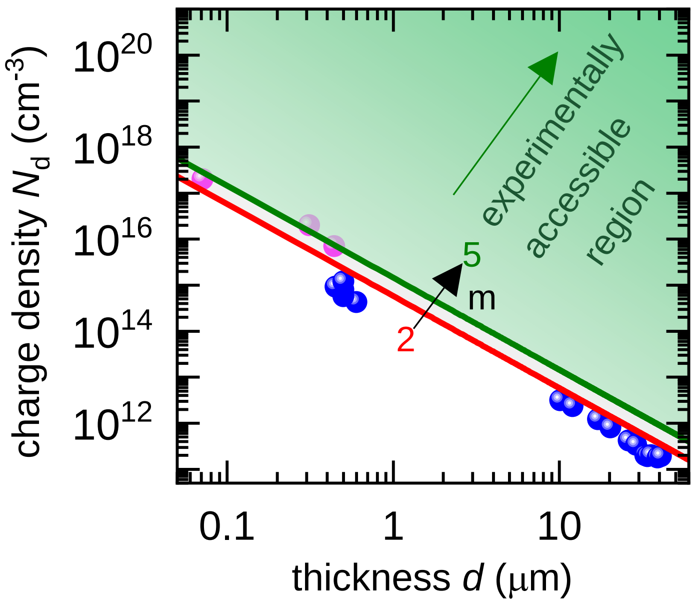

apparent minimum trap densities below resolution limit →

$$N_{\mathrm{d,min}} = \frac{27 m k_{\mathrm{B}} T \epsilon_{\mathrm{r}} \epsilon_0}{4 q^2 d^2}$$

Ravishankar, S., Unold, T. and Kirchartz, T., 2021. Comment on “Resolving spatial and energetic distributions of trap states in metal halide perovskite solar cells”. *Science*, *371*(6532).

doping profile – multilayer model

$$C(V) = C_\mathrm{g} + C_0 \exp\frac{qV}{mk_\mathrm{B}T} \longrightarrow N_\mathrm{d}(w) = N_\mathrm{d,min} + \frac{mk_\mathrm{B}T\epsilon_\mathrm{r}\epsilon_0}{q^2w^2}$$

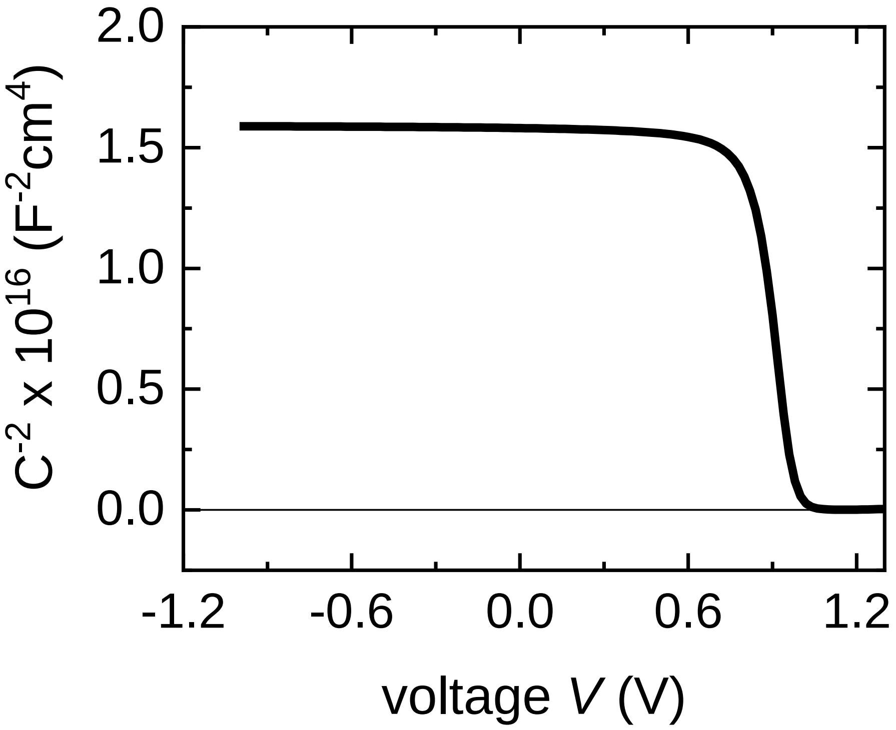

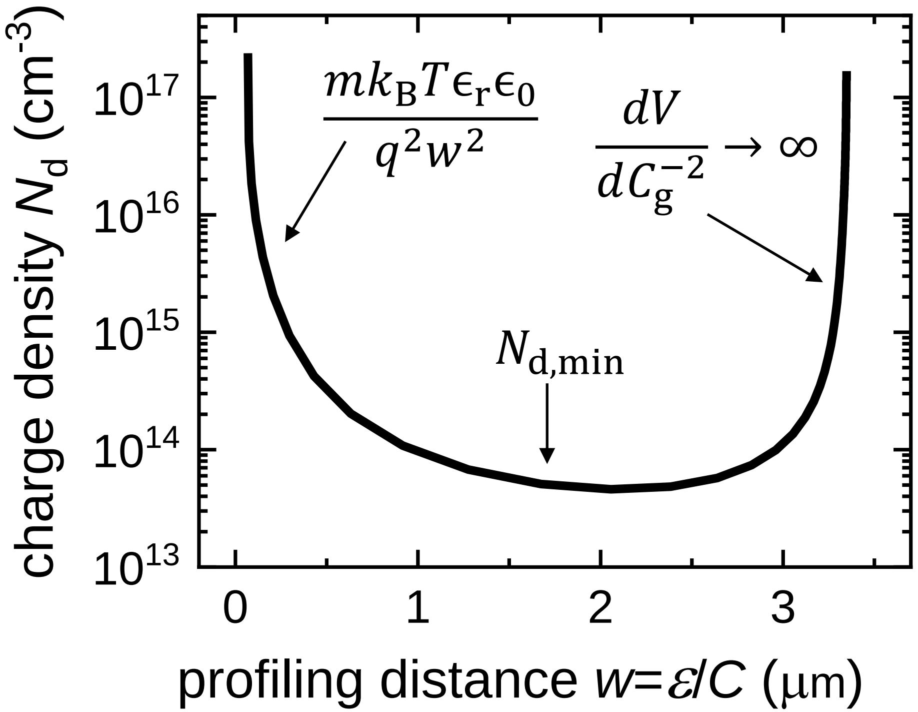

Ravishankar, S., Unold, T. and Kirchartz, T., 2021. Comment on “Resolving spatial and energetic distributions of trap states in metal halide perovskite solar cells”. *Science*, *371*(6532).

doping profiles of other photovoltaic technologies

Prof. Thomas Unold, Helmholtz Zentrum, Berlin

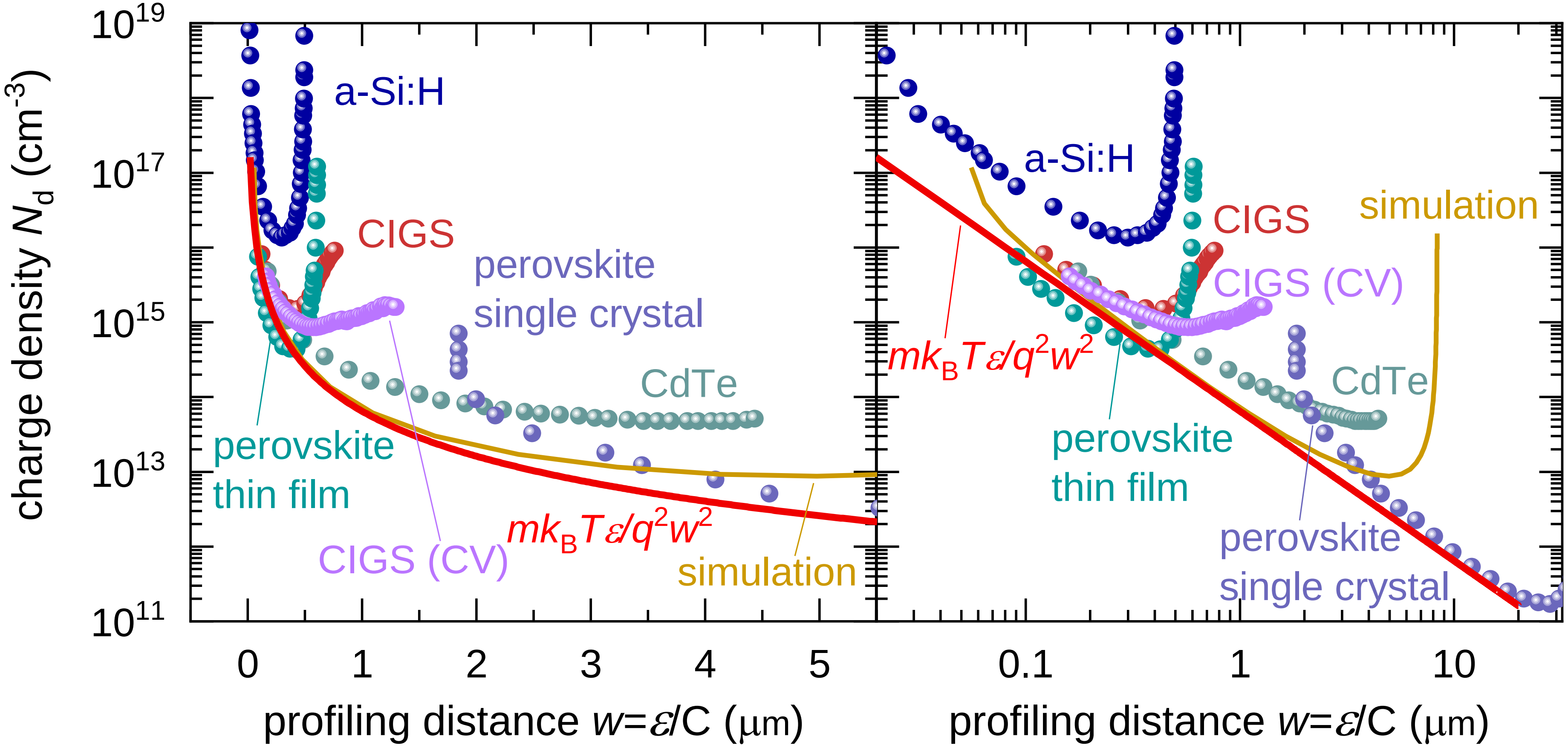

Ravishankar, S., Unold, T. and Kirchartz, T., 2021. Comment on “Resolving spatial and energetic distributions of trap states in metal halide perovskite solar cells”. *Science*, *371*(6532).

thermal admittance spectroscopy (TAS)

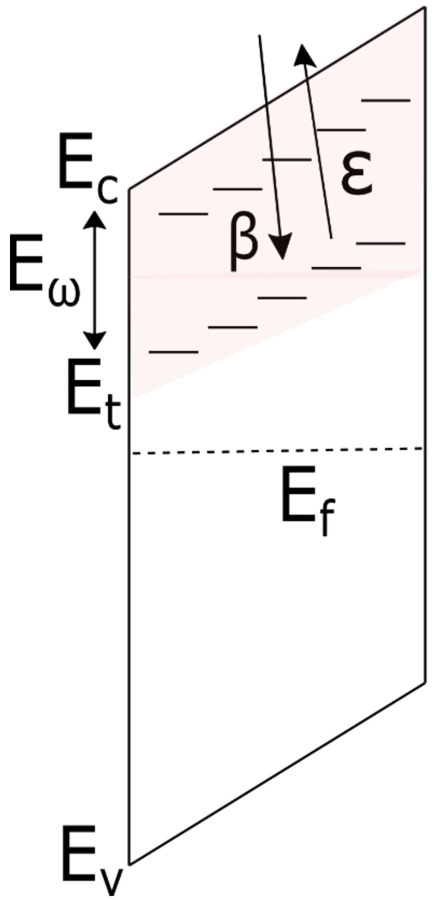

$$\omega_{\mathrm{td}} = \beta\bar{n} + \varepsilon = \beta\bar{n}[1 + \exp(\frac{E_{\mathrm{t}} - E_{\mathrm{f}}}{k_{\mathrm{B}}T})]$$

For $\frac{E_{\mathrm{t}}-E_{\mathrm{f}}}{k_{\mathrm{B}}T} \gg 1$, $\omega_{\mathrm{td}} = \beta N_{\mathrm{c}}\exp(\frac{-E_{\omega}}{k_{\mathrm{B}}T})$

$$C_{\mathrm{trap}}(\omega) = \frac{qd}{\tilde{V}} \frac{\omega_{\mathrm{td}}}{\omega^2 + \omega_{\mathrm{td},0}^2} \beta N_{\mathrm{t}}(1 - \bar{f})\tilde{n}$$

$$\frac{d^2 C_{\mathrm{trap}}}{d\omega^2} = 0 \to \omega_{\mathrm{td},0} \to \ln\left(\frac{\omega_{\mathrm{td},0}}{\beta(\propto T^2)N_{\mathrm{c}}}\right) = \frac{-E_{\omega}}{k_{\mathrm{B}}T}$$

$$\ln\left(\frac{\omega_{\mathrm{inflection}}}{T^2}\right) = \ln k - \frac{E_{\omega}}{k_{\mathrm{B}}T}$$

slope of inflection frequency/T^2 versus $1/k_BT$ yields the activation energy

Walter, T., Herberholz, R., Müller, C. and Schock, H.W., 1996. Determination of defect distributions from admittance measurements and application to Cu (In, Ga) Se2 based heterojunctions. *Journal of Applied Physics*, *80*(8), pp.4411-4420.

experiment

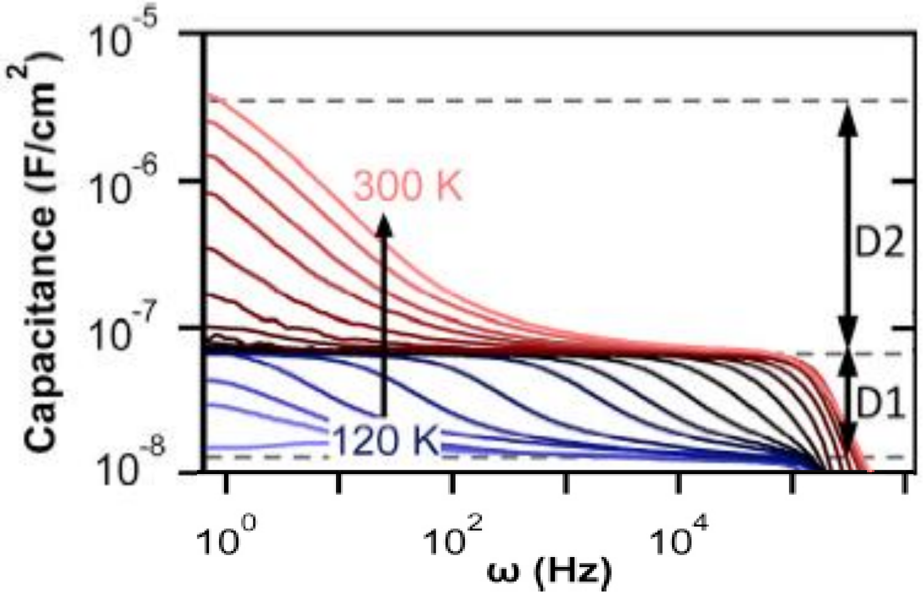

multilayer model

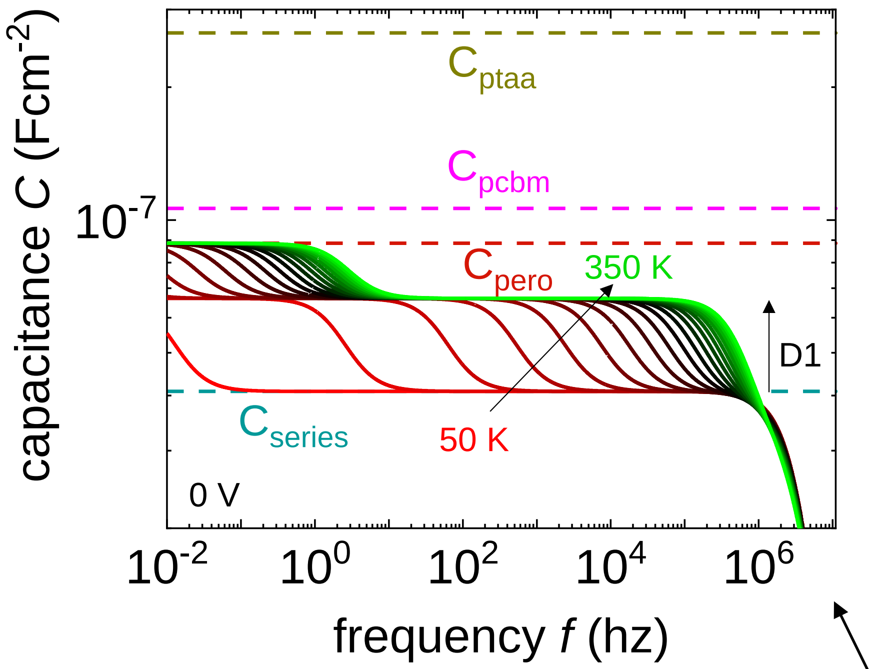

'D1' step ascribed to trapping-detrapping of free carriers, 'D2' step ascribed to ionic process

$$R_{\mathrm{ETL}}, R_{\mathrm{HTL}} \propto \frac{1}{k_{\mathrm{B}}T}\exp\left(\frac{q(V_{\mathrm{bi,TL}}-V)}{mk_{\mathrm{B}}T}\right)$$

Awni, R.A., Song, Z., Chen, C., Li, C., Wang, C., Razooqi, M.A., Chen, L., Wang, X., Ellingson, R.J., Li, J.V. and Yan, Y., 2020. Influence of charge transport layers on capacitance measured in halide perovskite solar cells. *Joule*, *4*(3), pp.644-657.

general RC transition - TAS

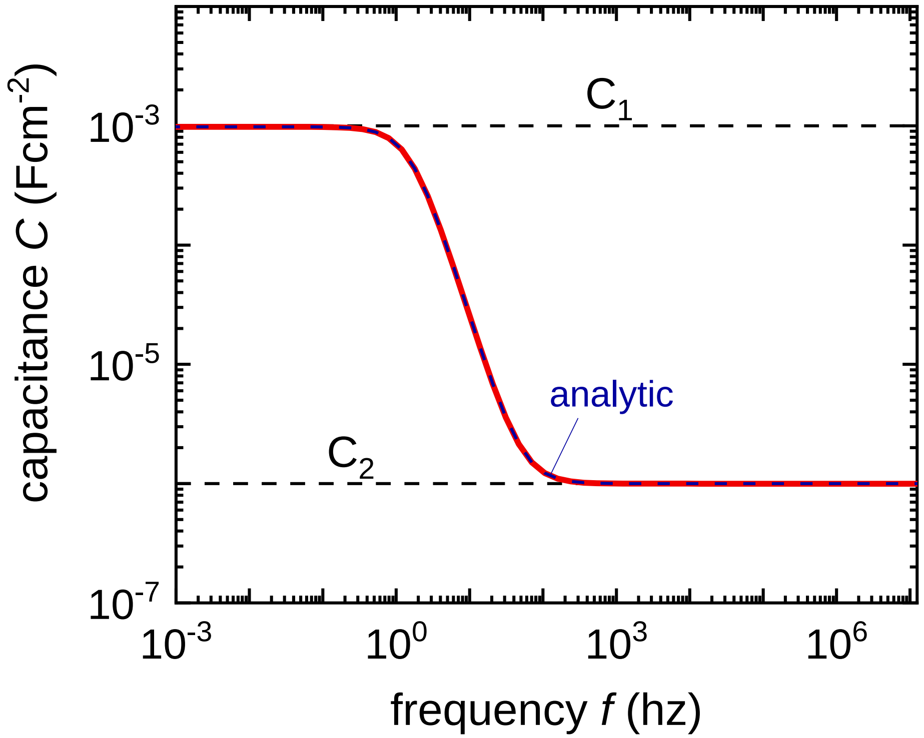

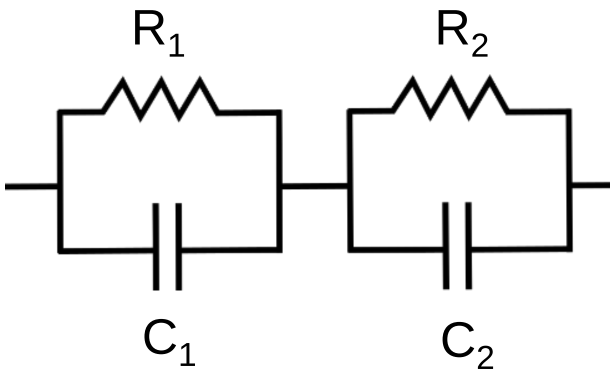

$$C(\omega) = C_2 + \frac{\left(\frac{R_1}{R_{\text{eff}}}\right)^2 C_1}{\left(\frac{R_1 + R_{\text{eff}}}{R_{\text{eff}}}\right)^2 + \left(\frac{\omega}{\omega_1}\right)^2}$$

$$R_{\text{eff}} = R_1(\alpha - 1) + R_2 \longrightarrow \alpha = \sqrt{\frac{R_1^2 C_1}{R_1^2 C_1 + R_2^2 C_2}}$$

$$\omega_{inf}(\alpha = 1) = \frac{1}{\sqrt{3} R_{||} C_1}$$

$$R_{\mathrm{ETL}}, R_{\mathrm{HTL}} \propto \frac{1}{k_{\mathrm{B}}T}\exp\left(\frac{q(V_{\mathrm{bi,TL}} - V)}{mk_{\mathrm{B}}T}\right) \longrightarrow \omega_{\mathrm{inf}} \propto \frac{1}{k_{\mathrm{B}}T}\exp\left(-\frac{q(V_{\mathrm{bi,TL}} - V)}{mk_{\mathrm{B}}T}\right)$$

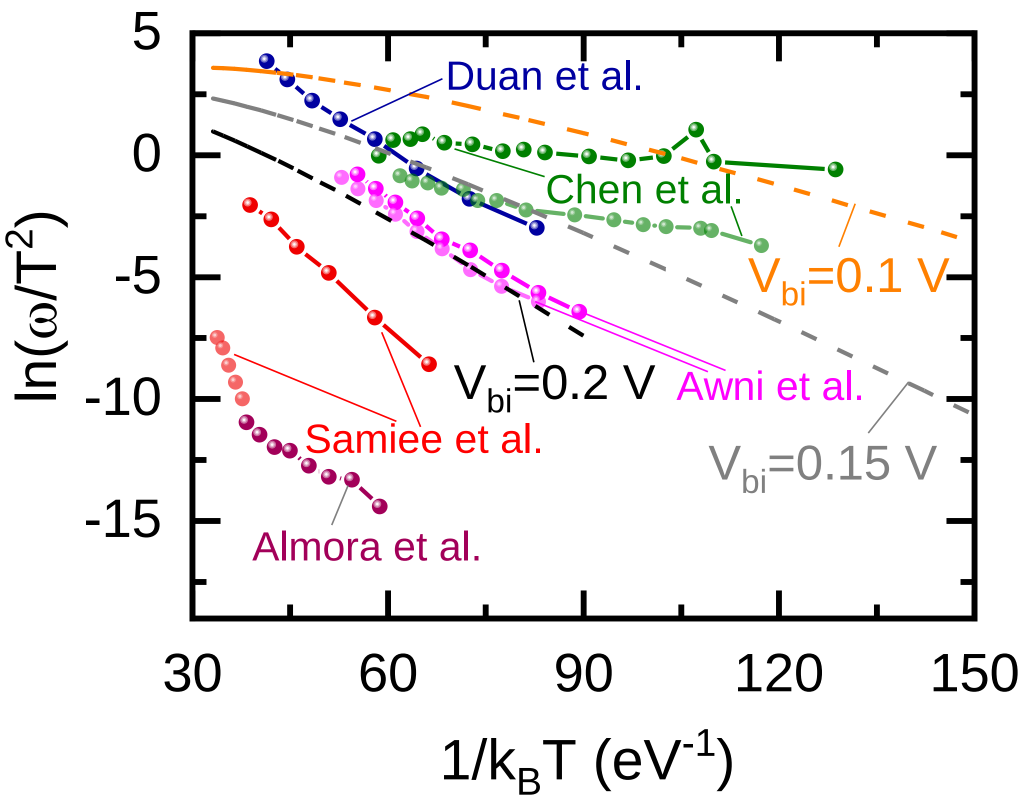

$$E_{\mathrm{A}} = \frac{V_{\mathrm{bi,TL}}}{m} - 3k_{\mathrm{B}}T$$

Awni et al., *Joule*, 2020, *4*(3).
Almora, O. et al., 2019. *J. Phys. Chem. Lett.* *10*(13).
Duan, H.S. et al., 2015. PCCP, *17*(1), pp.112-116.
Chen, Q. et al., *Nat. Commun.*, 2015, *6*(1).
Samiee, M. et al., 2014, *Appl. Phys. Lett.*, *105*(15).

time domain

$$C(\omega) = C_0 + \frac{\alpha\tau}{1+(\omega\tau)^2} \longrightarrow C(t) = C_0 + \alpha\exp(\frac{-t}{\tau})$$

general RC transition

$$C(\omega) = C_0 + \frac{\left(\frac{R_1}{R_{\mathrm{eff}}}\right)^2 C_1}{\left(\frac{R_1+R_{\mathrm{eff}}}{R_{\mathrm{eff}}}\right)^2 + \left(\frac{\omega}{\omega_1}\right)^2}$$

trap capacitance

$$C(\omega) = C_0 + \frac{qd}{\tilde{V}}\frac{\omega_{\mathrm{td}}}{\omega^2+\omega_{\mathrm{td,0}}^2}\beta N_{\mathrm{t}}(1-\bar{f})\tilde{n}$$

$$\longrightarrow C(\omega) = C_0 + \frac{a}{b+(\omega\tau)^2} \longrightarrow C(\omega) = C_0 + \frac{(\frac{a}{\sqrt{b}\tau})\frac{\tau}{\sqrt{b}}}{1+(\omega\frac{\tau}{\sqrt{b}})^2}$$

Ershov, M., Liu, H.C., Li, L., Buchanan, M., Wasilewski, Z.R. and Jonscher, A.K., 1998. Negative capacitance effect in semiconductor devices. *IEEE Transactions on Electron devices*, *45*(10), pp.2196-2206.

deep-level transient spectroscopy (DLTS), transient ion-drift (TID) $\longrightarrow$ $C(t) = C_0 \mp \alpha \exp(\frac{-t}{\tau})$ $\longrightarrow$ $\frac{1}{\tau} \propto \exp(\frac{-E_A}{k_B T})$

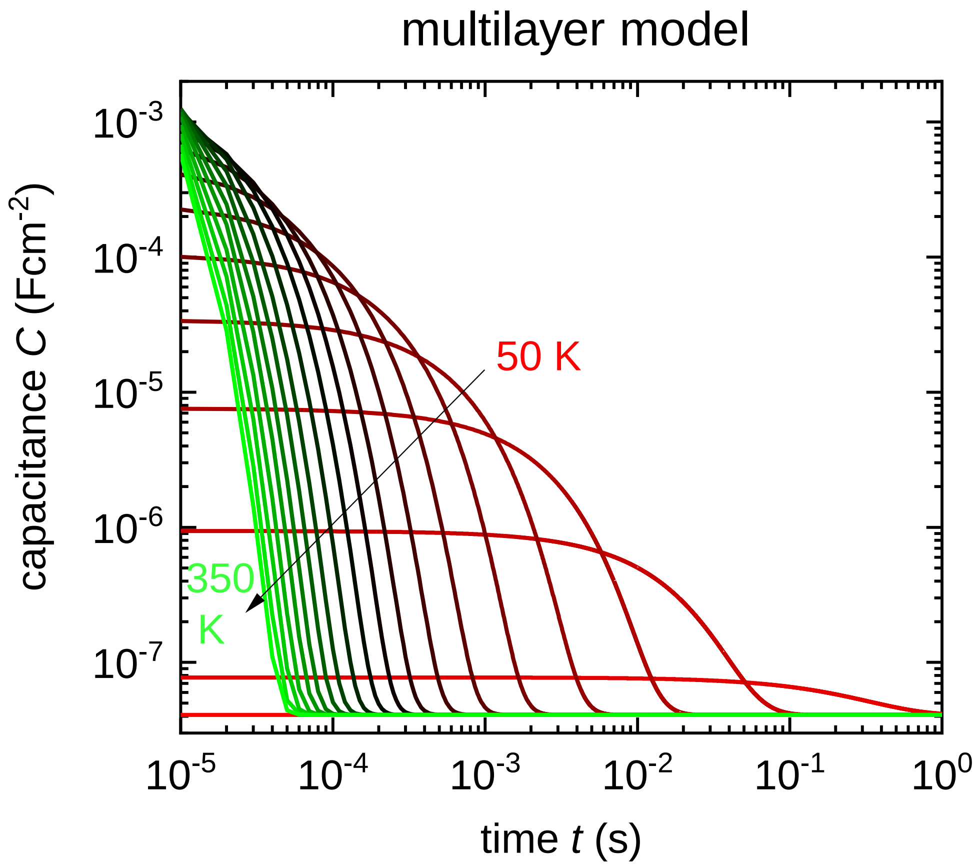

difficult to differentiate between ionic diffusion, trapping-detrapping and a general RC transition

conclusions

Capacitance measurements on devices will yield a minimum response from the selective contacts that depends on the resistance of the layers.

Capacitance models of PSCs should include the capacitance and resistance of the selective contacts.

acknowledgements

Dr. Zhifa Liu, Forschungszentrum Jülich

Dr. Jingjing Liu, Forschungszentrum Jülich

Helmholtz association, PEROSEED project

Thank you for your attention